Fabrication of PDMS-Based Microfluidic Devices: Application for Synthesis of Magnetic Nanoparticles

Vu Thi Thu, An Ngoc Mai, Le The Tam, Hoang Van Trung, Phung Thi Thu, Bui Quang Tien, Nguyen Tran Thuat & Tran Dai Lam

Journal of Electronic Materials

ISSN 0361-5235

Journal of Elec Materi
DOI 10.1007/s11664-016-4424-6

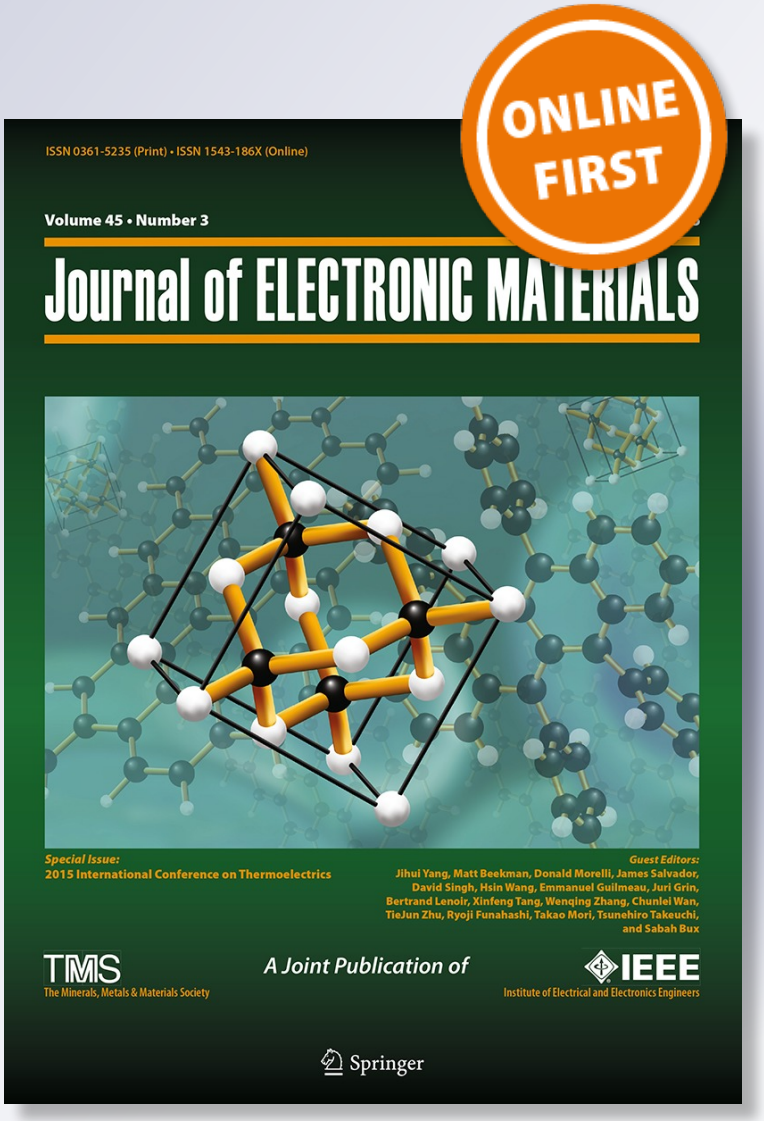

Springer

Journal of ELECTRONIC MATERIALS
DOI: 10.1007/s11664-016-4424-6

Fabrication of PDMS-Based Microfluidic Devices: Application for Synthesis of Magnetic Nanoparticles

VU THI THU,[1,7] AN NGOC MAI,[1] LE THE TAM,[2] HOANG VAN TRUNG,[3] PHUNG THI THU,[3] BUI QUANG TIEN,[4] NGUYEN TRAN THUAT,[5] and TRAN DAI LAM[4,6,8,9]

1.—University of Science and Technology of Hanoi, 18 Hoang Quoc Viet, Cau Giay, Hanoi, Vietnam. 2.—Vinh University, 182 Le Duan, Vinh, Nghe An, Vietnam. 3.—Institute of Materials Science, Vietnam Academy of Science and Technology, 18 Hoang Quoc Viet, Cau Giay, Hanoi, Vietnam. 4.—Graduate University of Science and Technology, Vietnam Academy of Science and Technology, 18 Hoang Quoc Viet, Cau Giay, Hanoi, Vietnam. 5.—Hanoi University of Science, 334 Nguyen Trai, Thanh Xuan, Hanoi, Vietnam. 6.—Duy Tan University, 182 Nguyen Van Linh, Da Nang, Vietnam. 7.—e-mail: thuvu.edu86@gmail.com. 8.—e-mail: trandailam@gmail.com. 9.—e-mail: tdlam@gust-edu.vast.vn

In this work, we have developed a convenient approach to synthesize magnetic nanoparticles with relatively high magnetization and controllable sizes. This was realized by combining the traditional co-precipitation method and microfluidic techniques inside microfluidic devices. The device was first designed, and then fabricated using simplified soft-lithography techniques. The device was utilized to synthesize magnetite nanoparticles. The synthesized nanomaterials were thoroughly characterized using field emission scanning electron microscopy and a vibrating sample magnetometer. The results demonstrated that the as-prepared device can be utilized as a simple and effective tool to synthesize magnetic nanoparticles with the sizes less than 10 nm and magnetization more than 50 emu/g. The development of these devices opens new strategies to synthesize nanomaterials with more precise dimensions at narrow size-distribution and with controllable behaviors.

Key words: Microfluidic, microreactor, magnetic nanoparticles, co-precipitation

INTRODUCTION

Magnetic nanoparticles have become increasingly attractive in the past few decades due to their promising potential in biomedical imaging,[1] drug delivery,[2] tumor hyperthermia,[3] biosensing,[4] and tissue engineering.[5] For a given application, it is critical to control the size, magnetization, as well as the surface coating of magnetic particles in order to determine their effectiveness. Indeed, these key parameters of magnetic platforms can be tuned through appropriate synthetic procedures.[1] Several synthesis methods for magnetic nanoparticles have been reported in the literature, mainly including co-precipitation,[6–8] thermal decomposition,[9–11] microwave assistance,[12] sono assistance,[13] and laser ablation.[14] Among these methods, the co-precipitation approach to date represents the best compromise with a wide range of advantages such as the use of cheap chemicals, mild and water-based reaction mediums, and easy surface functionalization.[1] High-energy approaches offer better control in size of magnetic particles.[9–14] Despite their considerable advantages, these traditional methods pose challenges to highly precise control in size and properties of magnetic particles. Thus, the development of a new strategy for synthesis of magnetite particles is still highly desirable for newly emerging biomedical applications.

In recent years, microfluidic systems have emerged as an attractive technology for nanoparticles synthesis.[15] These systems enable the automation and high-precision control of reaction

(Received December 17, 2015; accepted February 20, 2016)

Published online: 08 March 2016

conditions; therefore, tuey provide higher levels of control of particle size and their properties. Another important feature of microfluidic technology lies in the high reproducibility due to the limitations of manual handling. Very importantly, synthetic procedure can be scaled up by integrating a number of similar microsystems in parallel, thereby increasing the yield of the desired product. In the last decade, the use of the microfluidic approach for nanoparticle synthesis extended to a variety of materials of any nature including semiconductor,[16] metals,[17] polymers,[18] and metal–organic frameworks (MOFs).[19] Only a few works reported the use of microfluidic systems to synthesize magnetite particles.[20,21] The development of complete device for synthesizing high-quality materials has attracted much attention these days.

The main purpose of our present work is to demonstrate a simple and convenient approach for synthesis of nanometer-sized magnetite particles in a continuous process. The use of simplified microfabrication techniques enables low-cost manufacturing procedures of devices. The spatial confinement and automated manipulation of liquid flow in microfluidic devices will probably enable high-precision control in size and properties of the materials. The product properties were assessed through morphology and magnetization, measured using field emission scanning electron microscopy (FESEM) and a vibrating sample magnetometer (VSM), respectively. The very first results gained here will be of value in development of continuous large-scale manufacture of nanomaterials in the near future.

EXPERIMENTAL

Materials

Silicon wafers (3 inches in diameter, *p*-type, ⟨111⟩) and SU-8 2050 photoresists were purchased from MicroChem. Inc., (USA). Poly (dimethylsiloxane) (PDMS) and curing agent (SYLGARD 184 Silicone Elastomer) were purchased from Dow Corning Inc., (USA). Ferrous chloride ($FeCl_2$) and ferric chloride ($FeCl_3$) were purchased from Sigma-Aldrich. Sodium hydroxide and sulfuric acid were purchased from Sigma-Aldrich. Acetone and isopropanol were purchased from Merck Inc., (Germany).

Apparatus

The photolithography process was performed on a mask aligner system OAI (OAI, Taiwan). The activation of PDMS and glass surfaces was conducted on a Pico Diener oxygen plasma oven (Diener, Germany). A syringe pump (Razel, France) was used to inject the liquid flows into the device.

Conceptual Design

The configuration of the microfluidic device is represented in Fig. 1. Basically, the device consists of a serpentine micromixer, two inlets and one outlet (1.6 mm diameter). The two liquid inlets lead reagents into a micromixer where the reacting chemicals can be mixed together. The final product will be gained at the outlet.

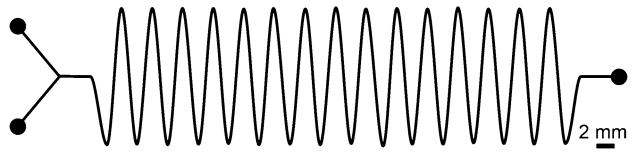

Fig. 1. Conceptual design of microfluidic device for continuous synthesis of magnetic nanoparticles. The diameter of inlets and outlet is 1.6 mm. The height and depth of the serpentine mixer are 15 mm and 50 mm, respectively.

Fabrication of PDMS-Based Microfluidic Devices

PDMS-based microfluidic devices were fabricated using a basic process flow in solf-lithography as described in Fig. 2. A SU-8 photoresist mold was first created using photolithography, then used to mold a PDMS pattern, and finally the PDMS fluidic part was sealed with a glass platform using oxygen plasma. The detailed process will be described in the following sections.

Mold Preparation

The photoresist mold was prepared using recommended photolithography program provided by Microchem. Inc., for a SU-8 2050 photoresist. In photolithography (from step i to step vi), the geometric patterns from a photo-mask were transferred on a photoresist film after a short exposure under UV light. The transparent photomasks with designed patterns were printed on a local hand-out printer and then fixed on a glass square fixture (5 × 5 inches). The exposure time was increased three times (5 s) to ensure the same luminescence power was lighted to photoresist film as compared to a chrome mask. The depth of the fluidic patterns are determined from the thickness of SU-8 photoresist film.

PDMS Casting

The PDMS fluidic part was cast from the above photoresist mold (step vii and step viii). A mixture containing PDMS base and curing agent (base/curing agent = 10/1) was poured onto the mold. The PDMS part was peeled off from the mold after annealing at 110°C for 1 h.

Bonding

Plasma oxygen bonding technique was used to stick PDMS fluidic part to a clean glass platform (step ix). The plasma conditions were 150 W and 90 s. A thermal treatment at 110°C for 1 h was required to strengthen the adhesion between PDMS and glass materials.

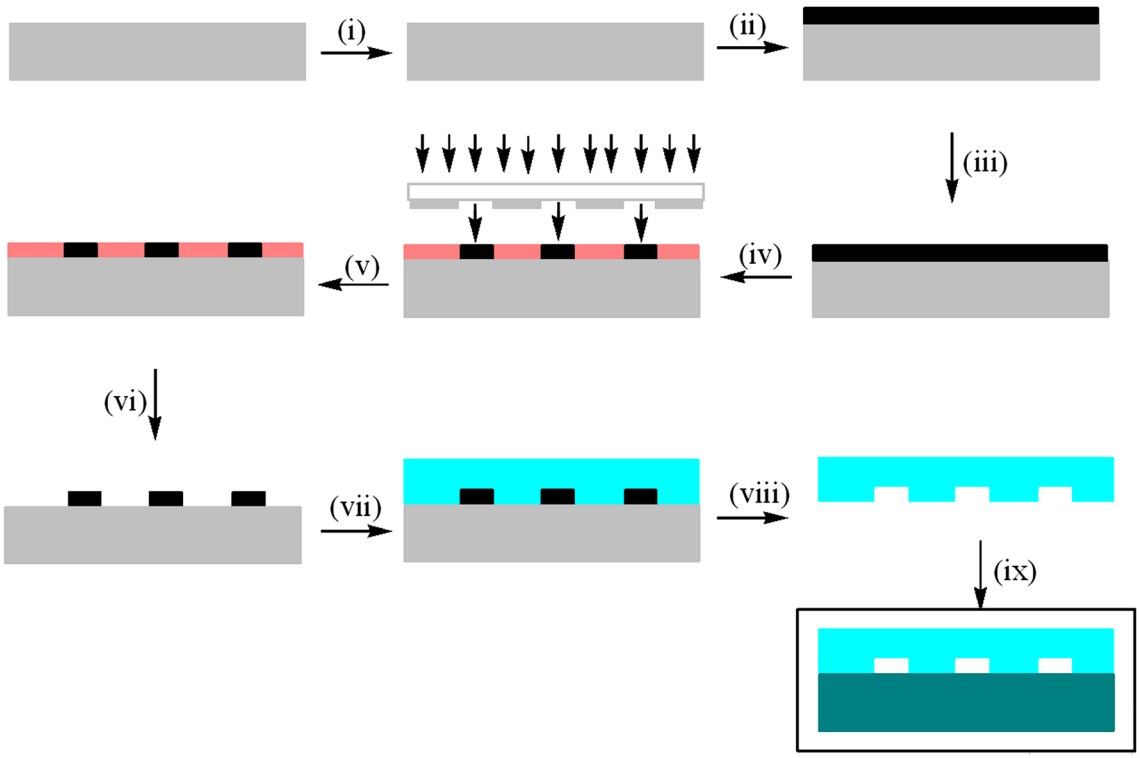

Fig. 2. Process flow to fabricate PDMS-based microfluidic device: (i) substrate pretreatment; (ii) deposition of photoresist on silicon substrate; (iii) pre-baking; (iv) exposure; (v) post-baking; (vi) developing; (vii) modeling; (viii) peeling off; (ix) bonding PDMS fluidic part to glass platform using oxygen plasma.

Synthesis of Magnetic Nanoparticles

2 M $FeCl_2$ and 1 M $FeCl_3$ solutions were prepared in HCl 1 M. The mixture of iron (II) and iron (III) acidic solutions were injected into the device at one inlet while 5 M NaOH solution was injected into the device from the other inlet. The molar ratio $[Fe^{2+}]/[Fe^{3+}]$ was 1/2. The flow rate was set to be 1 ml/h. The formation of magnetic particles was indicated by the appearance of a dark precipitate that could be attracted easily by an external magnet. The final product was washed several times with deionized water, then washed with ethanol and finally dried at 60°C for 2 h.

Characterization of Magnetic Nanoparticles

The morphology of the samples was observed by Ultra high resolution scanning electron microscopy with a (FESEM) Hitachi-S4800. The saturation magnetization of the samples at room temperature was measured under the highest magnetic field of 10 kOe using a vibrating sample magnetometer.

RESULTS AND DISCUSSION

PDMS-Based Microfluidic Device

Figure 3 shows an optical image of a device observed under the camera of an iPhone 5. It can be seen that the device was manufactured with desired structure. The zoomed images of well-defined patterns of the device were also observed under an optical microscope (data not shown here). The depth of the microchannels was assumed to be the same as that with the SU-8 mold. The stylus profile (Fig. 4) indicated that the device depth is around 20 μm and almost the same at different edges.

Fig. 3. An image of a PDMS-based microfluidic device (observed under the camera of an iPhone 5).

It must be emphasized that we used a transparent photomask instead of a chrome mask. In general, the PDMS patterns were cast from photoresist molds, which were prepared by photolithography using a chrome photomask.[22] Herein, the chrome photomask was replaced with a transparent photomask. That means there is no need to conduct

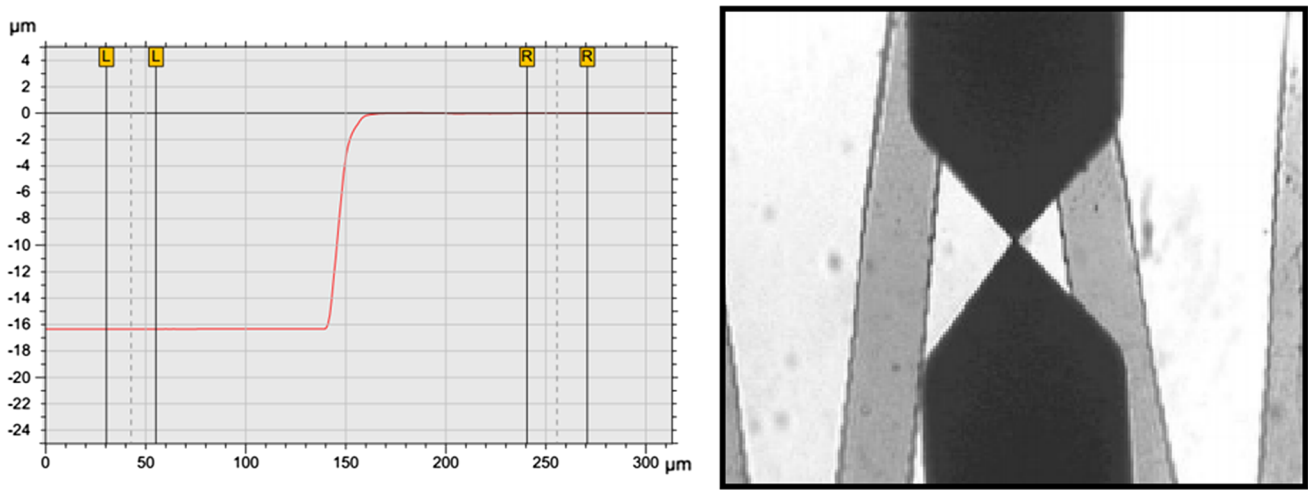

Fig. 4. Geometry of SU-8 mold observed under a stylus profiler.

expensive, time-consuming, and multi-steps procedures to prepare the photomask for the lithography process in our case. The total time to prepare the mask was about 1 h. The mask manufacturing cost was dramatically decreased from 500 USD/100 cm^2 for chrome mask down to 0.3 USD/100 cm^2 for our mask. This process can generate well-defined micropatterns smaller than 20 μm.

The stability of the device was tested with increasing flow rates. The results demonstrated strong adhesion of the fluidic part onto our glass platform and no water leakage was obtained within the working flow rates ranging from 1 to 10 ml/h. The treatment of PDMS and glass with oxygen plasma generated hydrophilic surfaces by introducing silanol groups (-Si-OH) and removing methyl groups ($-CH_3$).[23] This allows a better binding to silicate glass surfaces and a formation of an irreversible seal to create leak-tight channels.

The mixing performance of the device was tested with using two color dyes as samples. A complete mixing of the two injected liquids was visibly observed. The needed time to mix completely the two liquids is only within several minutes. The fast and effective mixing in the micromixer would be very important to ensure contact between reactants in a chemical synthesis.

Magnetic Nanoparticles

The co-precipitation of ferrous and ferric ions was conducted in 20-μm deep devices at a molar ratio of Ferric/Ferrous = 1/2. The formation of iron oxide magnetic particles inside microfluidic devices was indicated by the formation of dark precipitates. Evidently, this precipitate can be quickly attracted to the bottom of a baker under an external magnetic field due to high magnetization of the obtained products.

Figure 5 represents a FESEM image of magnetic particles obtained in microfluidic devices. It can be

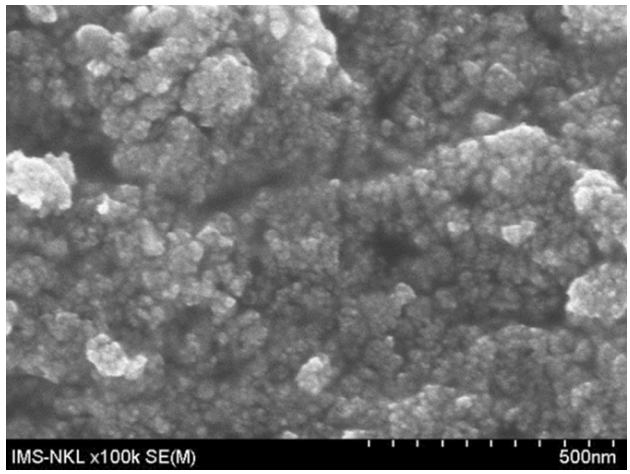

Fig. 5. The SEM image of the magnetic iron oxides particles prepared in the micro-channel.

seen that the particles were formed in spherical shape with relatively small diameter (about 10 nm). It was believed that the use of a microreactor can produce smaller and more uniform nanoparticles. One unique feature of microfluidic technology is the capacity to address reacting chemicals in a laminar regime flow in which liquid streams run in parallel paths.[24] This is the reason why microfluidic technology enables precise control of the size of nanoparticles. It was reported in the literature that the use of heating, microwave or sono assistance, and additives can help to narrow the size distribution of nanoparticles.[12–14] Here, the use of the microfluidic approach allows achieving high-precision control of particle size without using such energy sources.

Magnetic properties of the synthesized magnetic particles were characterized using a vibrating sample magnetometer (VSM). Figure 6 shows the room-temperature magnetization hysteresis loops of magnetite particles. Under a large external field, the

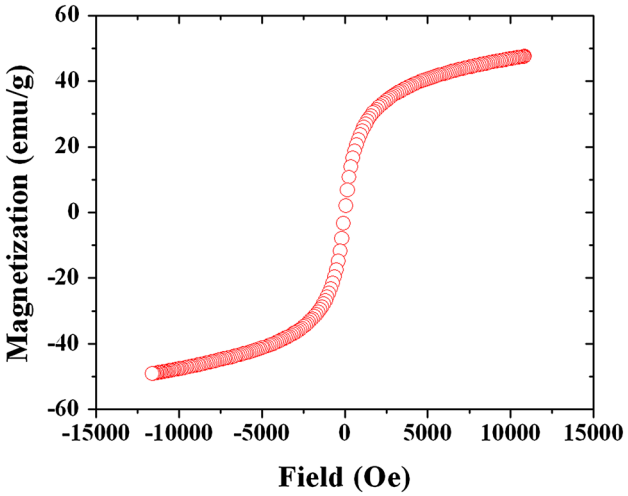

Fig. 6. The magnetization curve of the magnetic particles prepared in the micro-channel at molar ratio Fe^{3+}/Fe^{2+} = 1/2.

magnetizations of all magnetic domains align with the field direction and reach their saturation value. The maximal magnetization was determined (from the magnetization curve) to be 50 emu/g. However, it must be noticed that the real value saturation magnetization must be higher than the practical value for small magnetic particles (less than 10 nm) due to particle size effects.[25] The exact value of saturation magnetization should be further determined from the law of approach saturation.[25]

The relatively high value of magnetization is in agreement with our previous observations. Nevertheless, the desired saturation magnetization of magnetic particles for biomedical applications such as a magnetic resonance image (MRI) and hyperthermia treatment must be more than 70 emu/g.[11,26–28] Thus, the device configuration and experimental conditions need to be improved in our further works to gain better quality of the materials.

The batch-preparation of magnetite particles was also performed at the same conditions at room temperature. In comparison to the characteristics of magnetic iron oxide nanoparticles formed in batch-synthesis (data not shown here), the ones formed inside the micro-channel have a smaller size and higher magnetization.

CONCLUSION

A simple microfluidic system capable of mixing and controlling reaction conditions was developed for synthesis of magnetic nanoparticles. The usual soft-lithography techniques were simplified to lower the manufacturing cost of the microfluidic systems and satisfy low-resource conditions at our laboratory. Compared with batch-synthesis, the continuous synthesis in microfluidic devices helps to accelerate and automate the synthesis of iron oxide nanoparticles. Consequently, magnetite nanoparticles with smaller size, better size distribution, and improved magnetic behavior were observed. The size of the obtained particles was about 10 nm and the saturated magnetization was more than 50 emu/g. In our future work, drop-let based microfluidic devices with improved configurations will be developed to synthesize nanoparticles with selective sizes. The other nanomaterials (crystal nanomaterials, metal nanoparticles, MOFs and so on…) will be the next objectives.

ACKNOWLEDGEMENTS

This work received financial support from the Vietnam Academy of Science and Technology (VAST 03.01/15-16) and National Foundation for Science and Technology Development (NAFOSTED, 104.04-2014.36). This work was partly funded by University of Science and Technology of Ha Noi (Nano 1).

REFERENCES

1. T.-H. Shin, Y. Choi, S. Kima, and J. Cheon, *Chem. Soc. Rev.* 44, 4501 (2015).
2. L.D. Tran, N.M.T. Hoang, T.T. Mai, H.V. Tran, N.T. Nguyen, T.D. Tran, M.H. Do, Q.T. Nguyen, D.G. Pham, T.P. Ha, H.V. Le, and P.X. Nguyen, *Colloid. Surf. A* 371, 104 (2010).
3. A.E. Deatsch and B.A. Evans, *J. Magn. Magn. Mater.* 354, 163 (2014).
4. N.N. Thinh, P.T.B. Hanh, T.V. Hoang, V.D. Hoang, L.H. Dang, N.V. Khoi, and T.D. Lam, *Mater. Sci. Eng. C* 33, 1214 (2013).
5. S. Gil and J.F. Mano, *Biomater. Sci.* 2, 812 (2014).
6. M.C. Mascolo, Y. Pei, and A. Terry, *Materials* 6, 5549 (2013).
7. J.S. Basuki, A. Jacquemin, L. Esser, Y. Li, C. Boyer, and T.P. Davis, *Polym. Chem.* 5, 2611 (2014).
8. S. Wu, A. Sun, F. Zhai, J. Wang, W. Xu, Q. Zhang, and A.A. Volinsky, *Mater. Lett.* 65, 1882 (2011).
9. S. Sun and H. Zeng, *J. Am. Chem. Soc.* 124, 8204 (2002).
10. K. Woo, J. Hong, S. Choi, H.-W. Lee, J.-P. Ahn, C.S. Kim, and S.W. Lee, *Chem. Mater.* 16, 2814 (2004).
11. M.G.- Weimuller, M. Zeisberger, and K.M. Krishnan, *J. Magn. Magn. Mater.* 321, 1947 (2009).
12. W.-W. Wang, Y.-J. Zhu, and M.-L. Ruan, *J. Nanopart. Res.* 9, 419 (2007).
13. N. Wang, L. Zhu, D. Wang, M. Wang, Z. Lin, and H. Tang, *Ultrason. Sonochem.* 17, 526 (2010).
14. J. Zhang, M. Post, T. Veres, Z.J. Jakubek, J. Guan, D. Wang, F. Normandin, Y. Deslandes, and B. Simard, *J. Phys. Chem. B* 110, 7122 (2006).
15. S. Marre and K.F. Jensen, *Chem. Soc. Rev.* 39, 1183 (2010).
16. E.M. Chan, A.P. Alivisatos, and R.A. Mathies, *J. Am. Chem. Soc.* 127, 13854 (2005).
17. V.S. Cabeza, S. Kuhn, A.A. Kulkarni, and K.F. Jensen, *Langmuir* 28, 7007 (2012).
18. J. Puigmartí-Luis, M. Rubio-Martínez, U. Hartfelder, I. Imaz, D. Maspoch, and P.S. Dittrich, *J. Am. Chem. Soc.* 133, 4216 (2011).
19. M. Faustini, J. Kim, G.-Y. Jeong, J.Y. Kim, H.R. Moon, W.-S. Ahn, and D.-P. Kim, *J. Am. Chem. Soc.* 135, 14619 (2013).
20. L. Frenz, A.E. Harrak, M. Pauly, S. Begin-Colin, A.D. Griffiths, and J.-C. Baret, *Int. Ed. Angew. Chem.* 47, 6817 (2008).
21. W.B. Lee, C.H. Weng, F.Y. Cheng, C.S. Yeh, H.Y. Lei, and G.B. Lee, *Biomed. Microdevices* 11, 161 (2009).
22. D. Qin, Y. Xia, and G.M. Whitesides, *Nat. Protoc.* 5, 491 (2010).
23. J. Zhou, A.V. Ellis, and N.H. Voelcker, *Electrophoresis* 31, 2 (2010).

24. G.M. Whitesides, *Nature* 442, 368 (2006).
25. L.L. Balcells, J. Fontcuberta, B. Martinez, and X. Obradors, *Cond. Matt.* 10, 1883 (1998).
26. B. Mehdaoui, A. Meffre, J. Carrey, S. Lachaize, L.-M. Lacroix, M. Gougeon, B. Chaudret, and M. Respaud, *Adv. Func. Mater.* 21, 4573 (2011).
27. T.T. Luong, T.P. Ha, L.D. Tran, M.H. Do, T.T. Mai, N.H. Pham, H.B.T. Phan, G.H.T. Pham, N.M.T. Hoang, Q.T. Nguyen, and P.X. Nguyen, *Colloid. Surf. A* 384, 23 (2011).
28. T.K.O. Vuong, D.L. Tran, T.L. Le, D.V. Pham, H.N. Pham, T.H.L. Ngo, H.M. Do, and X.P. Nguyen, *Mater. Chem. Phys.* 163, 1 (2015).